Analyst

Cite this: *Analyst*, 2012, **137**, 5785

www.rsc.org/analyst

PAPER

Catalytic activity and stability of glucose oxidase/horseradish peroxidase co-confined in macroporous silica foam

Xiaodong Cao, Ying Li, Zhiqiang Zhang, Jiachao Yu, Jing Qian and Songqin Liu*

Received 3rd September 2012, Accepted 1st October 2012
DOI: 10.1039/c2an36237f

Investigation of the catalytic activity and stability of enzymes in confined nano/microspace provides valuable contributions to the fundamental understanding of biological reactions taking place on a mesoscopic scale within confined spaces. In this paper, macroporous silica foam (MSF) is used as a nanoreactor to co-confine glucose oxidase (GOD) and horseradish peroxidase (HRP). Then, the enzymatic cascade reactions, which act in tandem inside nanoreactors, for oxidation of glucose and 3,3′,5,5′-tetramethylbenzidine (TMB) were studied. The catalytic kinetic parameters of apparent Michaelis constant (K_m^{app}) and maximum rate (V_{max}) were obtained from Lineweaver–Burk plot by UV-vis spectrometry. Results showed that the catalytic activity of the co-confined enzymes is reduced compared to that of free enzymes in solution at room temperature. The stabilities of co-confined enzymes in denaturing agents, such as guanidinium chloride (GdmCl) and urea, were higher than those of free enzymes in solution. When employing a co-confined bienzyme system as a biosensor for the detection of glucose, a wider linear range of glucose was obtained for the co-confined bienzyme system than for free enzymes in solution.

Introduction

Recently, three-dimensional porous materials with highly ordered porous structure, large surface area, and tight pore size distributions have been widely used as nano/microreactors for confinement of biomolecules and applied in biotechnology including protein adsorption and immobilization,[1–3] dug delivery,[4] biosensing,[5,6] and proteolysis.[7,8] Especially, the silica-based porous materials have received promising attention due to their ordered structure, uniform pore size, and friendly environment for proteins.[9] The ease of modification of the inside pore walls provide silica-based porous materials which confine biomolecules by new routes. The inside walls of silica-based porous materials can be modified with functional groups, –CHO, for instance, for covalent immobilization of proteins;[10] or with metal oxides by using simple impregnation and calcination processes, changing the surface charge of inside walls, for adsorption and immobilization of proteins by electrostatic interactions.[7,8,11,12]

Macroporous silica foam (MSF), synthesized from a block-copolymer vesicle templating method, has been applied in protein immobilization and adsorption,[1] and protein proteolysis for proteomics.[7,8] The immobilization capacities of MSF and other mesoporous materials (mesocellular foams, and rodlike SBA-15) were studied using bovine serum albumin (BSA, $M = 67$ kDa) as the guest molecules. The equilibrium adsorption amount of BSA for MSF, mesocellular foams, and rod-like SBA-15 was 251, 134, and 104 mg g^{-1}, respectively. MSF showed superior bioimmobilization capacity over other porous materials for biomolecules with large molecular weight, suggesting that MSF with high pore volumes and large pore sizes are much better candidates for the immobilization of large biomolecules.[1] Surface modification of MSF has been used as multi-functional nano-reators.[7,8] Typically, there are three functions for surface modified MSF: firstly, the macropores are applied as nanoreactors for enzymatic reactions; secondly, the nanoreactors accelerate protein digestion by quick enrichment of enzymes and proteins in the macropores without increasing the enzyme/protein concentration or using a preimmobilization process; lastly, the nanoreactors could *in situ* isolate specific products of the enzymatic reaction and release the nonspecific peptides to the solution due to the chemo-affinity between chemical modified groups of MSF surface and specific groups of the detecting proteins.

As many natural biological reactions, such as enzymatic reactions, take place on a mesoscopic scale in confined space, interest in understanding the catalytic activity and stability of proteins or enzymes confined in nano/microreactors has risen. Studies on pH for enzyme immobilization in mesoporous silica pores show a large influence on both the maximum adsorbed amount[13,14] and activity of enzymes.[14] Pore size of mesoporous silica is a key factor that affects the activity of the enzyme confined in the mesopores.[14,15] Takahashi *et al.* discovered that immobilized HRP on FSM-16 and MCM-41 with pore diameter

School of Chemistry and Chemical Engineering, Southeast University Jiangning, Nanjing 211189, People's Republic of China. E-mail: liusq@seu.edu.cn; Fax: +86-25-52090618; Tel: +86-25-52090613

50 Å that matched the molecular diameters of the enzyme showed the highest enzymatic activity in an organic toluene and better thermal stability than other mesoporous silica materials with large or small pore size.[15]

Conformational stability of protein investigation is normally applied with denaturing agents guanidinium chloride (GdmCl) and urea, which has been extended to proteins/enzymes confined in mesoporous silica materials.[2,16,17] When confining hemoglobin in mesoporous silica (FSM: folded-sheet mesoporous material) with pore diameter of 7.5 nm, the resistance towards GdmCl was much better than the free enzyme in solution due to protein inflexibility in the mesopores.[17] Lei *et al.*[16] concluded that it was the synergetic effects of functionalized mesoporous silica and urea that promoted favorable protein conformational changes, and thus enhanced specific activity of glucose isomerase entrapped in FMS in the presence of denaturing agent urea. The activity of entrapped enzyme remained high in presence of 8.0 M urea, while that of free enzymes in solution was totally lost.

In the present work, MSF was skillfully synthesized and utilized as nanoreactors for co-confining glucose oxidase (GOD) and horseradish peroxidase (HRP). The enzyme cascade reaction occurring inside the nanoreactors was investigated in detail by using glucose and 3,3′,5,5′-tetramethylbenzidine (TMB) as substrates. It was demonstrated that the catalytic activity of co-confined enzymes was reduced compared free enzymes in solution, while good stability of the co-confined enzymes was achieved.

Experimental

Chemicals and instrumentation

Tetramethyl orthosilicate (TMOS), glucose oxidase (GOD, EC 1.1.3.4, from *Aspergillus niger*, 181.3 kU g^{-1}), and poly(ethylene oxide)–poly(propylene oxide)–poly(ethylene oxide) ($EO_{20}PO_{70}EO_{20}$, M_n = 5800, denoted P123, product of Germany) were purchased from Sigma-Aldrich Chemical Co. 3,3′,5,5′-Tetramethylbenzidine (TMB), guanidinium chloride (GdmCl) and horseradish peroxidase (HRP, EC 1.11.1.7, RZ ≥ 3.0, 250 U mg^{-1}) were obtained from Nanjing Sunshine Biotechnology Co., Ltd. (Jiangsu, China). Anhydrous sodium sulfate (Na_2SO_4), acetic acid (HAc), sodium acetate anhydrous (NaAc) were purchased from Sinopharm Chemical Reagent Co., Ltd. (Shanghai, China). All other chemicals were of analytical grade and used without further purification. Phosphate buffer solution (PBS) was prepared by mixing NaH_2PO_4 and Na_2HPO_4. Twice-distilled water was used throughout the study.

Transmission electron microscope (TEM) images were obtained using a Tecnai G2 instrument operated at 200 kV (FEI, Netherlands). Before the measurements, 10 μL of samples dispersed in water was dropped onto copper grids and dried in vacuum overnight. A field emission scanning electron microscope (SEM, ULTRA PLUS, ZEISS, Germany) at an acceleration voltage of 5 kV was used to obtain SEM images of MSF. 10 μL of samples well dispersed in water were dropped onto clean silicon slices and dried in vacuum overnight prior to the measurements being taken. The intensity of enzymatic cascade reaction with color change was measured on a UV-1102 UV-vis spectrophotometer (Techcomp, Shanghai, China).

Synthesis of MSF

MSF was synthesized according to the procedures reported by Yu's group with a little modification.[18] Typically, 0.5 g of P123 was dissolved in 15 mL 0.02 M pH 5.0 NaAc–HAc buffer solution to form a homogenous solution under stirring. 0.78 g of tetramethyl orthosilicate (TMOS) was added to this solution and stirred for 5 min. The resulting mixture was kept under static conditions for 24 h at 35 °C and hydrothermally treated at 100 °C for another 24 h. The precipitate was filtered, washed with water, and dried in air. The final product was obtained by calcination at 550 °C for 5 h.

Adsorption of GOD and HRP in MSF

The mixture solution of GOD and HRP (500 μL) was added to 5 mg MSF placed in a centrifuge tube. The mixture was gently stirred at 4 °C for 48 h. The solution was then centrifuged and washed several times with phosphate buffer until no free enzyme in the supernatant could be detected. The adsorption amount of GOD and HRP into the macropores was calculated by subtracting the unadsorbed enzymes from the total amount of enzymes monitored by UV-vis spectra. The materials GOD + HRP/MSF were stored at 4 °C.

Assays of enzyme activity

The catalytic kinetic assays using UV-vis spectra methods were carried out at room temperature in 2 mL PBS (0.1 M, pH 5.5). For the kinetic assay of TMB, 50 μL glucose (0.1 M), and 2 μL mixture of GOD and HRP (0.930 mg mL^{-1} and 0.883 mg mL^{-1} in free buffer solution respectively) or GOD + HRP/MSF suspension (absorbed in 0.1 M PBS pH 5.5) were added to a 2 mL reaction buffer with varying concentrations of TMB. For the kinetic assay of glucose, 20 μL TMB (5×10^{-3} M), and 2 μL mixture of GOD and HRP (0.930 mg mL^{-1} and 0.883 mg mL^{-1} in a enzyme free buffer solution respectively) or GOD + HRP/MSF suspension (absorbed in 0.1 M PBS pH 5.5) were added to a 2 mL reaction buffer with varied concentrations of glucose. After the substrates were quickly mixed, the catalytic reaction was allowed for 30 min. All reactions were monitored by using a kinetic mode at 650 nm and the rates of the reactions were evaluated from the initial slopes of the time-dependent absorbance curves.

Stability in the presence of denaturing agents

180 μL of denaturing agents (0–5 M urea or 0–5 M GdmCl) was mixed with free GOD and HRP in buffer solution (20 μL, protein concentration: 0.930 mg mL^{-1} GOD; 0.883 mg mL^{-1} HRP) or the GOD + HRP/MSF (20 μL; absorbed in 0.1 M PBS pH 5.5) for 24 h at room temperature. Next, the samples (5 μL) were added to 2 mL PBS (0.1 M pH 5.5) containing 5×10^{-5} M TMB and 2.5 mM glucose. After the substrates were mixed, the catalytic reaction was allowed to stand for 1 min, and the absorbance was measured at 650 nm on UV-1102 UV-vis spectrophotometer.

GOD + HRP/MSF for the detection of glucose

Glucose detection using colorimetric methods was carried out with TMB as the chromogenic substrate. 5 μL mixture of GOD

and HRP (9.30 μg mL^{-1} and 8.83 μg mL^{-1} in enzyme free buffer solution, respectively) or GOD + HRP/MSF suspension (absorbed in 0.1 M PBS pH 5.5 diluted 100 times) were added to a 2 mL reaction buffer (pH 5.5) with varied concentrations of glucose. The mixture was allowed to stand for 1 min, and the absorbance was recorded at 650 nm on UV-1102 UV-vis spectrophotometer.

Results and discussion

MSF characterization

Normally, the unilamellar silica vesicles can be synthesized with cationic surfactants by utilizing either an equilibrium vesicle templating[19] or a cooperative vesicle templating process.[20] In our case, the triblock copolymer P123 was employed to form siliceous multilamellar vesicles through a cooperative vesicle templating process.[1,18,21] Fig. 1 was typical TEM and SEM images of MSF and hexagonally macropores could be clearly observed. The images showed the macroporous structures were about 100 nm in pore diameter, and the wall thickness was estimated to be 5 nm. The results obtained from TEM and SEM images were in good agreement with those from the literature.[7,8]

Enzyme immobilization and catalytic activity of the co-confined enzymes

GOD and HRP were simultaneously confined into the macropores of MSF by physical adsorption (Scheme 1A). The amount of enzymes adsorbed in MSF with different conditions are listed in Table 1. The amount of enzymes increased greatly with the increasing bulk concentration of enzymes from 1 to 5 mg mL^{-1}, and tended to increase slightly from 5 mg mL^{-1} to 8 mg mL^{-1} in pH 7.0 PBS. Therefore, the initial enzyme concentration for MSF adsorption was chosen to be 5 mg mL^{-1}. The amounts of enzymes adsorbed in MSF depended on the pH value in the GOD + HRP mixture solution. As we know that the isoelectric points of MSF, GOD, and HRP are about 2–4,[13,22] 3.8–4.5,[23–25] and 8.9,[26] respectively. Therefore, MSF exhibited a negative-charged surface at high pH solution, larger than pH 5.0, while GOD and HRP displayed different surface charge at around neutral solution. On the other hand, adsorption of enzymes is affected by two factors: one is electrostatic interactions between MSF and enzymes; the other is lateral interaction between enzyme molecules. Research has showed that the maximum adsorbed amount of enzymes will be achieved when pH is close to the isoelectric point of the protein.[2,13,25,27] Table 1 shows the

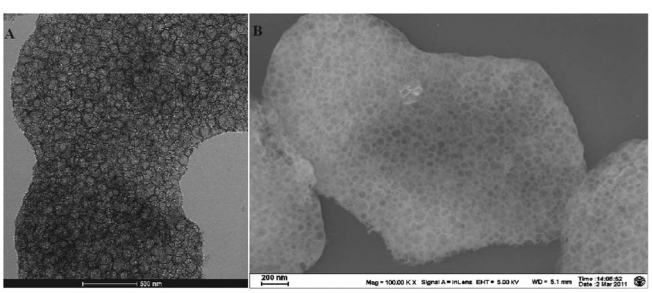

Fig. 1 TEM (A) and SEM (B) images of MSF.

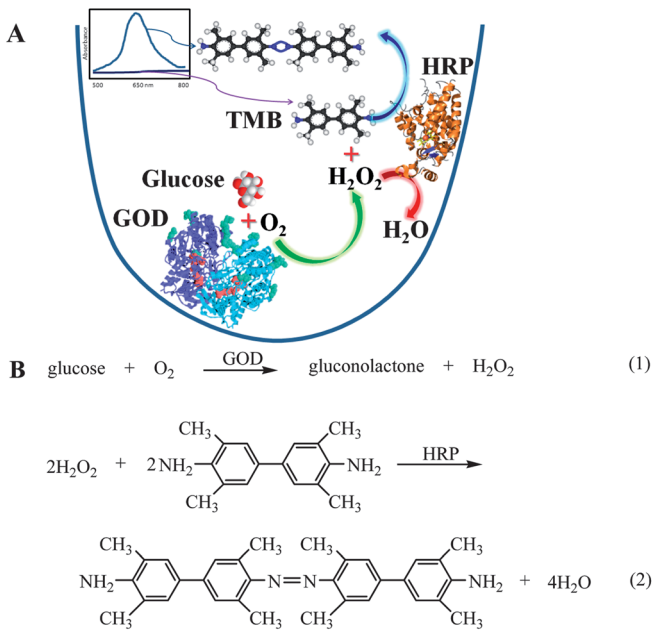

Scheme 1 (A) Schematic representation of enzymatic cascade reactions inside macropores of MSF. (B) Chemical reactions of the enzymatic cascade reactions.

amount of enzymes adsorbed in PBS at different pH. The amount of GOD absorbed decreased from pH 5.5 to 8.0, while the amount of HRP increased with increasing pH. The maximum adsorption of GOD and HRP occurred near the isoelectric point of proteins, which was in agreement with the literature.[2,13,25,27]

The catalytic activity of immobilized enzymes was investigated by UV-vis spectra using TMB as the colorimetric substrate.[28,29] In the presence of glucose and TMB, a cascade reaction catalyzed by GOD and HRP took place and is shown in Scheme 1B. The cascade reaction started with the oxidation of glucose catalyzed at ambient atmospheres and resulted the generation of $H_2O_2 \cdot H_2O_2$ product generated in the first step of the cascade reaction, oxidization of TMB with the catalysis of HRP into tetrazo compound, causimg a color change in the reaction buffer from clear to blue. This may be recorded on a UV-vis spectrophotometer for evaluation of enzyme catalytic activity.

The absorbance-time relations for enzymatic cascade reactions of oxidation glucose and TMB were carried out to first estimate enzyme activity (Fig. 2A). It is obvious that the reaction rates of the co-confined enzymes are much slower than those of enzymes in solution, while the initial rate of reactions is speeded up with

Table 1 Adsorption amounts of GOD and HRP into macropores under different conditions

pH	c_{GOD} and c_{HRP} in solution (mg mL^{-1})	GOD adsorption (mg)	Adsorption amount of HRP (mg)
7.0	1	0.115 ± 0.007	0.273 ± 0.0011
7.0	3	0.485 ± 0.014	0.760 ± 0.0160
7.0	5	0.806 ± 0.012	1.174 ± 0.012
7.0	8	0.819 ± 0.011	1.191 ± 0.016
5.5	5	0.930 ± 0.009	0.883 ± 0.011
6.3	5	0.873 ± 0.015	1.116 ± 0.009
8.0	5	0.560 ± 0.020	1.291 ± 0.012

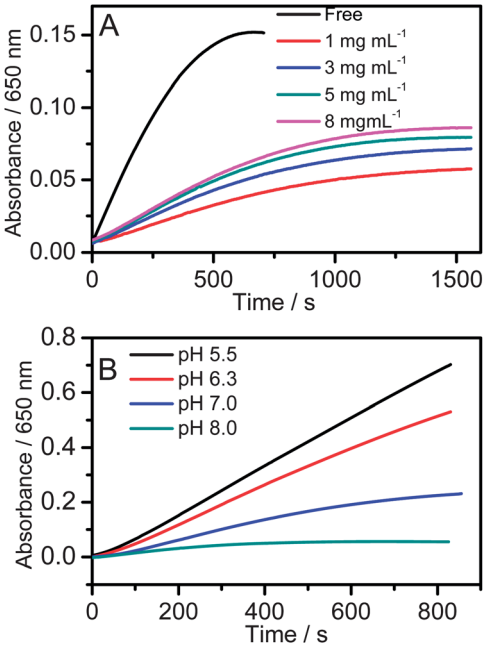

Fig. 2 (A) Time-dependent formation of tetrazo compound at room temperature in presence of GOD, HRP, and glucose using TMB as chromogenic substrate. *Reaction conditions*: 0.1 M PBS (pH 7.0); glucose concentration: 2.5×10^{-3} M; TMB concentration: 5×10^{-5} M. Note: the concentrations of GOD were the same throughout the experiments, while the concentrations of HRP were varied. (B) Time-dependent formation of tetrazo compound at room temperature catalyzed by GOD and HRP adsorbed into macropores of MSF in various pH. *Reaction conditions*: glucose concentration: 2.5×10^{-3} M; TMB concentration: 5×10^{-5} M. pH values of adsorbing buffer and detecting buffer were the same.

increasing amount absorbed in MSF. It was noted that only a slight increase of the initial rate occurred while changing the initial enzyme concentration from 5 to 8 mg mL^{-1}, which showed the same trend as the adsorbed amount of enzymes in MSF. The pH value of reaction buffer had a strong influence on enzyme activity. For example, the pH value for maximum GOD activity and stability is 5.0–6.0, and the activity and stability of GOD will be sharply reduced when pH value is higher than 7.0.[30,31] When adsorption of enzymes occurred in PBS at pH 5.5 and was detected in the same buffer, the enzymatic cascade reaction showed that the highest initial reaction rate (Fig. 2B). The bienzyme system co-confined in MSF absorbed in pH 5.5 PBS was used for the kinetic parameters calculating, stability evaluating, and glucose detecting.

In most cascade reactions, such as 6-phosphogluconate dehydrogenase and gluconate kinase in glucose oxidase/gluconate kinase/6-phosphogluconate dehydrogenase tandem,[32] and lactoperoxidase in superoxide dismutase/actoperoxidase tandem,[33] the Michaelis constant K_m^{app} and the maximum rate constant V_{max} were determined from Lineweaver–Burk or directly from Michaelis–Menten plots for evaluation of the enzyme catalytic kinetics. Herein, the Lineweaver–Burk approach was used to find the kinetic parameters for the cascade reaction of free enzymes and those inside macropores of MSF (Fig. 3, Table 2). The apparent K_m^{app} and the apparent V_{max} values were calculated by using TMB and glucose as substrates, respectively. Table 2 summarizes the catalytic constants obtained

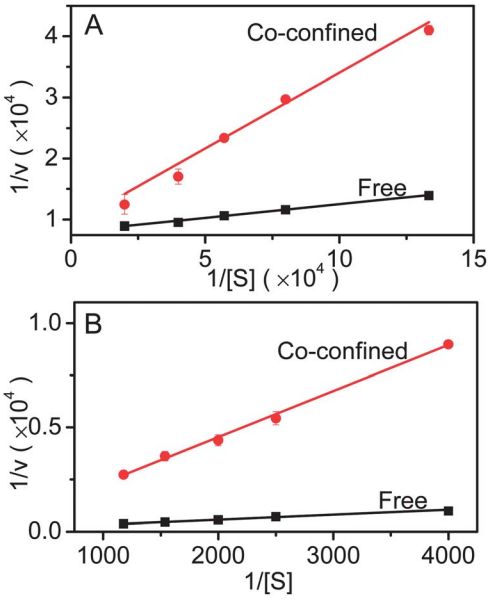

Fig. 3 (A) The Lineweaver–Burk plots for the GOD + HRP/MSF with TMB as a substrate. The concentration of glucose was 2.5×10^{-3} M. (B) The Lineweaver–Burk plots for the GOD + HRP/MSF with glucose as a substrate. The concentration of TMB was 5×10^{-5} M.

from Lineweaver–Burk plots. The results showed that K_m^{app} of free enzymes were lower than that of co-confined, while V_{max} were higher than the latter, suggesting that the catalytic activity of co-confined enzymes was lower than that of free enzymes in bulk solution.

Several factors may count for the reduced catalytic activity and lower V_{max} of immobilized enzymes. The folding state of enzymes in confined space may differ from that of free enzymes in solution, which might be the responsible for lower catalytic activity. When confining HRP and GOD in macropores of MSF separately, the catalytic activity of single-confined HRP reduced much more significantly than the single-confined GOD compared to free HRP or GOD in solution (Fig. 4). Previous studies demonstrated that the strong electrostatic interactions between positively charged protein and negatively charged silica gel might induce part protein unfolding or disrupt the geometry of the entrance to the active site, which would result in a decrease in activities of the positively charged enzymes when confined in silica materials.[23,24,34] It was revealed that van der Waals forces in confined nanospaces might also contribute to protein structure rearrangement.[35] In this case, when positively charged HRP was confined in MSF, strong electrostatic interactions occurred between HRP molecules and the walls of MSF, so changing the conformation of HRP and leading to a sharp reduction in HRP

Table 2 Comparison of apparent catalytic constants of free and immobilized enzymes at room temperature

Substrate	Enzyme status	K_m (M)	V_{max} (M s^{-1})
TMB	Free	$(5.64 \pm 0.19) \times 10^{-6}$	1.25×10^{-4}
	Co-confined	$(2.68 \pm 0.13) \times 10^{-5}$	1.08×10^{-4}
Glucose	Free	$(2.61 \pm 0.24) \times 10^{-3}$	10.9×10^{-3}
	Co-confined	$(1.92 \pm 0.19) \times 10^{-2}$	8.68×10^{-3}

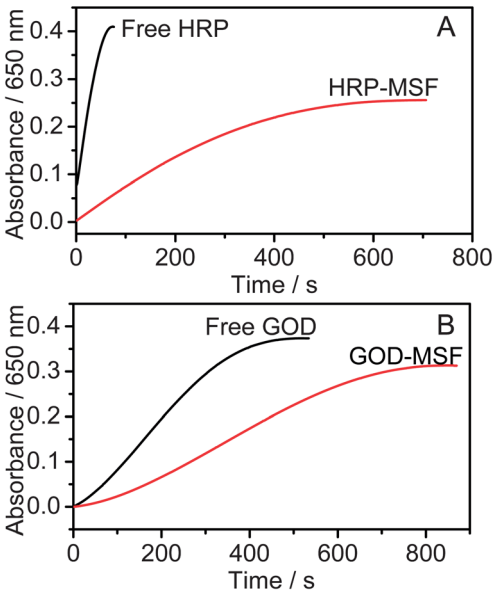

Fig. 4 (A) Time-dependent formation of tetrazo compound at room temperature in the oxidation of TMB by H_2O_2 catalyzed by HRP. *Reaction conditions*: 0.1 M PBS (pH 7.0); H_2O_2 concentration: 5×10^{-4} M; TMB concentration: 5×10^{-5} M; free HRP or confined HRP concentration: 4.6×10^{-10} M. Adsorbed amount of HRP in MSF (5 mg, 0.1 M pH 7.0 PBS) estimated to be 1.839 ± 0.021 mg. (B) Time-dependent formation of tetrazo compound at room temperature in presence of TMB, HRP, glucose, and free GOD or confined GOD in MSF. *Reaction conditions*: 0.1 M PBS (pH 7.0); TMB concentration: 5×10^{-5} M; glucose concentration: 2.5×10^{-3} M; free HRP concentration: 4.6×10^{-11} M, free GOD or confined GOD concentration: 1.5×10^{-8} M. Adsorbed GOD in MSF (5 mg, 0.1 M pH 7.0 PBS) was estimated to be 0.981 ± 0.024 mg.

activity. Besides, part of the active sites of GOD and HRP might be blocked due to lateral interactions between enzyme biomolecules, resulting in a reduction of enzymatic activity and a drop in V_{max}.

After being confined, the microlocal environment for enzymes, such as crowding effect and surface hydration, may be the second factor in reducing catalytic activity and lowering V_{max}.[36–39] Crowding effect[38] plays an important role in affecting the activity of enzymes and molecular diffusion rates. The effects of macromolecular crowding on suppressing the protease open state and reducing enzyme-ligand diffusional encounter rates likely combine to slow *in vivo* enzymatic activity. The macropores of MSF can serve as nanoreactors for GOD and HRP immobilization and enzymatic reactions of glucose and TMB oxidation. Activity of GOD and HRP in this crowded and confined environment will be reduced and show significant differences from that of free enzyme in dilute buffer solution. Moreover, reduced molecular (substrate/product) diffusion rates might result in the lower reaction rate of immobilized enzymes compared with free enzymes. Hydrogen bond strengthening and strengthened protein hydration are considered to be one of the causes of retarded activity of enzyme. It is generally believed that close proximity silanol groups at the silica surface influence the protein structure indirectly through changes in the hydrogen bonding properties of water, which may lead to increased hydration strength of the embedded protein.[39] As silanol groups exist at the MSF surface, hydrogen bonding may be strengthened, and thus the hydration of the co-confined enzymes in MSF strengthened as a result.

Stability in the presence of denaturing agents

Guanidine hydrochloride and urea are the most common chemical denaturants used for protein denaturation.[16,40] The stability of the immobilized enzymes against GdmCl and urea was investigated (Fig. 5). Immobilized enzymes retain a higher activity than free enzymes in aqueous solution after denaturing with GdmCl (Fig. 5A). Significant activity decrease is noted at 1 M GdmCl, followed by increased activity when GdmCl concentration increased from 1 M to 2 M. Further a strong decrease of enzyme activity is noted as the concentration of GdmCl is above 3 M. The reason for higher activity in 2 and 3 M GdmCl than in 1 M GdmCl may be due to a loosening up of the enzymes compact structure by GdmCl, resulting in increasing conformational flexibility especially at or near active sites.[41,42]

In contrast, immobilized enzymes denatured with urea showed much higher activity than free enzymes in aqueous solution (Fig. 5B). The activity of the immobilized enzymes dropped from 100% to 96% when the concentration of urea increased from 0 to

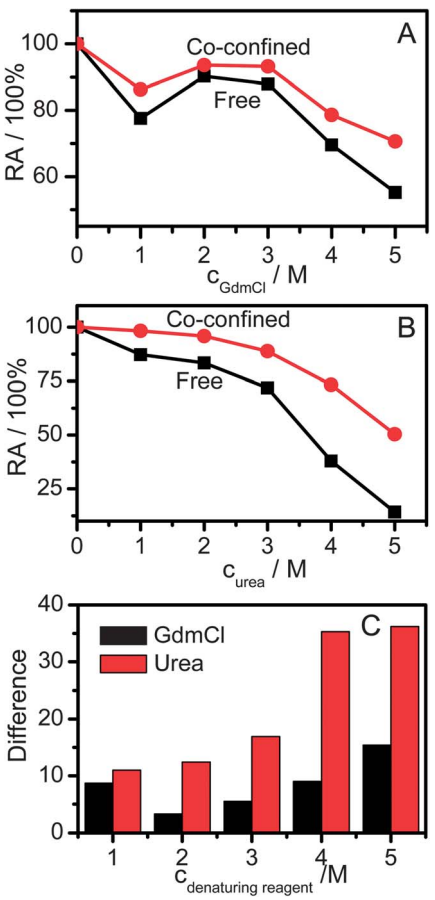

Fig. 5 Comparison of retained activity of free and immobilized enzymes after incubation with GdmCl (A) and urea (B); (C) the absolute difference of retained activity between immobilized and free enzymes denatured with GdmCl and urea.

2 M, *i.e.*, no significant change in enzymatic activity of the immobilized enzymes was observed up to 2 M urea. A sharp decrease in enzymatic activity was exhibited when the concentration of urea was between 2 and 5 M, especially in 4 M urea. However, the immobilized enzyme retained 50% activity in 5 M urea, whereas the activity of the free enzymes dropped to 14%.

The absolute difference of retained activity between immobilized and free enzymes denatured with urea was higher than that of those denatured with GdmCl (Fig. 5C). The precise denaturing mechanisms at the molecule level of GdmCl and urea are still unclear. Two models have been proposed for denaturant-dependent protein unfolding mechanisms: one is based on direct interaction between the denaturing agent and the protein, and the other is based on modification of the hydrogen-bonded structure of water and a consequent weakening of hydrophobic interactions.[2,40] Urea was found to interact directly with protein by pulling away water surrounding the protein, and result in perturbation of the structure of water simultaneously.[40] Consequently, protein unfolding took place because of both the direct interaction between urea and the protein and the variation of the structure of the solvent. GdmCl, on the other hand, acted directly on the protein without changing the static properties of the solvent around the proteins.[40] In the urea denaturing system, urea in the confined pore space cannot easily remove water near the pore wall. The motion of enzymes confined in MSF is therefore restrained. As a consequence, the retained activity of immobilized enzymes after urea denaturing is not as strongly affected as that of free enzymes in solution, and the relative difference of retained catalytic activity between immobilized and free enzymes is notable. In contrast, GdmCl acted directly on the protein without perturbation of the water structure. Combining the protein unfolding process mechanism in GdmCl with the interaction between enzymes and MSF walls, the relative difference of retained catalytic activity between immobilized and free enzymes is indistinct.

GOD + HRP/MSF for the detection of glucose

The bienzyme system was finally employed as a biosensor for the detection of glucose. A comparison between immobilized enzymes in MSF and free enzymes in solution is drawn by using colorimetric methods. Absorbance at 650 nm increased with glucose for both immobilized and free enzymes in solution under identical reaction conditions (Fig. 6). Absorbance increased with increasing glucose concentration until the highest absorbance for the enzymatic cascade reaction was reached for immobilized and free bienzyme system. Although the absorbance for the immobilized bienzyme system was lower than that of the free enzyme in solution at certain glucose concentrations, the immobilized bienzyme system showed a wide linear range towards glucose. Absorbance to glucose concentration for the immobilized bienzyme system showed a linear range from 5.0×10^{-5} to 1.0×10^{-2} M with a correlation coefficient of 0.986, while for the free enzyme in solution it ranged from 5.0×10^{-5} to 1.0×10^{-3} M with a correlation coefficient of 0.991. The broader linear range for glucose of the co-confined bienzyme system might be a result of the enzymes' reduced activity in the confined nanospace and lower reaction rate of the cascade reaction catalyzed by the co-confined enzymes. The result obtained for the co-confined bienzyme system as biosensor for detection of glucose is better than that for co-immobilized GOD and HRP in glass tubes, where the glucose concentration is linear in the range from 110 μM to 580 μM.[43]

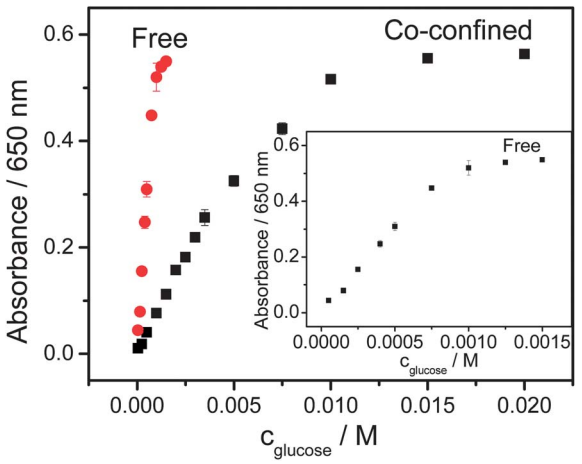

Fig. 6 Relationship between absorbance and glucose concentration. Inset: relationship between absorbance and glucose concentration in presence of free GOD and HRP. Concentration of TMB is 5×10^{-5} M.

Conclusions

We have employed macropores of MSF as nanoreactors for both co-confining GOD and HRP, and enzymatic cascade reaction for oxidation of glucose and TMB, which act in tandem inside nanoreactors. The comparison of catalytic activity between the immobilized enzymes and free enzymes in solution was investigated using UV-vis spectra. The catalytic activity of the immobilized enzymes at room temperature was lower than that of the free enzymes. The factors impacting on low catalytic activity of the immobilized enzymes are complicated. We assume that the differences, such as the folding state of enzymes and microlocal environment for enzymes, between immobilized enzymes and free enzymes in solution may be causes by different catalytic activity. Although the immobilized enzymes exhibit lower catalytic activity for oxidation of glucose and TMB, the use of the immobilized enzymes as a biosensor for detecting glucose showed a wider linear range than the free enzymes in solution. Stabilities towards the denaturing agents GdmCl and urea were also studied. The resistance of immobilized enzymes to GdmCl and urea was stronger than that of free enzymes in solution. The different mechanisms of protein folding processes in GdmCl and urea along with consequences of the interaction between enzymes and MSF walls may be responsible for the absolute differences between the immobilized enzymes and free enzymes in solution with GdmCl and urea as the denaturing agents.

Acknowledgements

The project is supported by the Key Program (21035002) from the National Natural Science Foundation of China, National Natural Science Foundation of China (Grant nos. 20875013, 21175021) and the Key Program (BK2010059) from the Natural Science Foundation of Jiangsu province, Open Foundation from

State Key Laboratory of Bioelectronics and Significant Scientific Research Guidance Foundation from Southeast University.

Notes and references

1 H. Wang, Y. Wang, X. Zhou, L. Zhou, J. Tang, J. Lei and C. Yu, *Adv. Funct. Mater.*, 2007, **17**, 613–617.
2 H. Ikemoto, Q. Chi and J. Ulstrup, *J. Phys. Chem. C*, 2010, **114**, 16174–16180.
3 A. Popat, S. B. Hartono, F. Stahr, J. Liu, S. Z. Qiao and G. Qing Max Lu, *Nanoscale*, 2011, **3**, 2801–2818.
4 A. Popat, J. Liu, Q. Hu, M. Kennedy, B. Peters, G. Q. Lu and S. Z. Qiao, *Nanoscale*, 2012, **4**, 970–975.
5 L. Zhang, *Biosens. Bioelectron.*, 2008, **23**, 1610–1615.
6 Z. Dai, J. Bao, X. Yang and H. Ju, *Biosens. Bioelectron.*, 2008, **23**, 1070–1076.
7 K. Qian, J. Wan, F. Liu, H. H. Girault, B. Liu and C. Yu, *ACS Nano*, 2009, **3**, 3656–3662.
8 K. Qian, J. Wan, X. Huang, P. Yang, B. Liu and C. Yu, *Chem.–Eur. J.*, 2010, **16**, 822–828.
9 S. Wu, H. X. Ju and Y. Liu, *Adv. Funct. Mater.*, 2007, **17**, 585–592.
10 L. Zhang, Q. Zhang and J. Li, *Biosens. Bioelectron.*, 2010, **26**, 846–849.
11 K. Yasutaka, Y. Takato, K. Takashi, M. Kohsuke and Y. Hiromi, *J. Phys. Chem. B*, 2011, **115**, 10335–10345.
12 K. Qian, J. Wan, L. Qiao, X. Huang, J. Tang, Y. Wang, J. Kong, P. Yang, C. Yu and B. Liu, *Anal. Chem.*, 2009, **81**, 5749–5756.
13 A. Vinu, V. Murugesan and M. Hartmann, *J. Phys. Chem. B*, 2004, **108**, 7323–7330.
14 W. Chouyyok, J. Panpranot, C. Thanachayanant and S. Prichanont, *J. Mol. Catal. B: Enzym.*, 2009, **56**, 246–252.
15 H. Takahashi, B. Li, T. Sasaki, C. Miyazaki, T. Kajino and S. Inagaki, *Chem. Mater.*, 2000, **12**, 3301–3305.
16 C. Lei, Y. Shin, J. Liu and E. J. Ackerman, *Nano Lett.*, 2007, **7**, 1050–1053.
17 Y. Urabe, T. Shiomi, T. Itoh, A. Kawai, T. Tsunoda, F. Mizukami and K. Sakaguchi, *ChemBioChem*, 2007, **8**, 668–674.
18 H. Wang, X. Zhou, M. Y. Wang, L. Han, J. Zhang, P. Yuan, G. Auchterlonie, J. Zou and C. Yu, *J. Am. Chem. Soc.*, 2006, **128**, 15992–15993.
19 H. P. Hentze, S. R. Raghavan, C. A. McKelvey and E. W. Kaler, *Langmuir*, 2003, **19**, 1069–1074.
20 S. Pevzner, O. Regev, A. Lind and M. Lindén, *J. Am. Chem. Soc.*, 2003, **125**, 652–653.
21 J. Zipfel, P. Lindner, M. Tsianou, P. Alexandridis and W. Richtering, *Langmuir*, 1999, **15**, 2599–2602.
22 V. Bansal, A. Syed, S. K. Bhargava, A. Ahmad and M. Sastry, *Langmuir*, 2007, **23**, 4993–4998.
23 Q. Chen, G. L. Kenausis and A. Heller, *J. Am. Chem. Soc.*, 1998, **120**, 4582–4585.
24 J. Heller and A. Heller, *J. Am. Chem. Soc.*, 1998, **120**, 4586–4590.
25 G. Ozyilmaz, S. S. Tukel and O. Alptekin, *J. Mol. Catal. B: Enzym.*, 2005, **35**, 154–160.
26 B. X. Gu, C. X. Xu, G. P. Zhu, S. Q. Liu, L. Y. Chen, M. L. Wang and J. J. Zhu, *J. Phys. Chem. B*, 2009, **113**, 6553–6557.
27 X. Wang, K. X. Zhu and H. M. Zhou, *Int. J. Mol. Sci.*, 2011, **12**, 3042–3054.
28 B. Li, Y. Du, T. Li and S. Dong, *Anal. Chim. Acta*, 2009, **651**, 234–240.
29 X. Cao, J. Yu, Z. Zhang and S. Liu, *Biosens. Bioelectron.*, 2012, **35**, 101–107.
30 L. T. Phuoc, P. Laveille, F. Chamouleau, G. Renard, J. Drone, B. Coq, F. Fajula and A. Galarneau, *Dalton Trans.*, 2010, **39**, 8511–8520.
31 G. Kenausis, Q. Chen and A. Heller, *Anal. Chem.*, 1997, **69**, 1054–1060.
32 Z. Zhu, C. Momeu, M. Zakhartsev and U. Schwaneberg, *Biosens. Bioelectron.*, 2006, **21**, 2046–2051.
33 P. Tanner, O. Onaca, V. Balasubramanian, W. Meier and C. G. Palivan, *Chem.–Eur. J.*, 2011, **17**, 4552–4560.
34 J. Livage, T. Coradin and C. Roux, *J. Phys.: Condens. Matter*, 2001, **13**, R673–R691.
35 D. E. B. Gomes, R. D. Lins, P. G. Pascutti, C. Lei and T. A. Soares, *J. Phys. Chem. B*, 2010, **114**, 531–540.
36 B. Menaa, Y. Miyagawa, M. Takahashi, M. Herrero, V. Rives, F. Menaa and D. K. Eggers, *Biopolymers*, 2009, **91**, 895–906.
37 H. Frauenfelder, P. W. Fenimore and B. H. McMahon, *Biophys. Chem.*, 2002, **98**, 35–48.
38 D. D. L. Minh, C. Chang, J. Trylska, V. Tozzini and J. A. McCammon, *J. Am. Chem. Soc.*, 2006, **128**, 6006–6007.
39 R. Ravindra, S. Zhao, H. Gies and R. Winter, *J. Am. Chem. Soc.*, 2004, **126**, 12224–12225.
40 C. Camilloni, A. Guerini Rocco, I. Eberini, E. Gianazza, R. A. Broglia and G. Tiana, *Biophys. J.*, 2008, **94**, 4654–4661.
41 Y. Fan, M. Ju, J. Zhou and C. Tsou, *Biochem. J.*, 1996, **315**, 97–102.
42 H. J. Zhang, X. R. Sheng, X. M. Pan and J. M. Zhou, *Biochem. Biophys. Res. Commun.*, 1997, **238**, 382–386.
43 S. Fornera, T. Bauer, A. D. Schlüter and P. Walde, *J. Mater. Chem.*, 2012, **22**, 502–511.